

^{23}Na spin-lattice relaxation of sodium nitrite in confined geometryS. B. Vakhrushev,* Yu. A. Kumzerov, A. Fokin, and A. A. Naberezhnov
*Ioffe Physico-Technical Institute, 26 Politekhnicheskaya, 194021, St. Petersburg, Russia*B. Zalar, A. Lebar, and R. Blinc
J. Stefan Institute, Jamova 39, 1000 Ljubljana, Slovenia

(Received 1 April 2004; revised manuscript received 19 May 2004; published 12 October 2004)

Whereas the ^{23}Na spin-lattice relaxation rate T_1^{-1} of microconfined NaNO_2 in the ferroelectric phase is similar to the one of bulk NaNO_2 , there is a striking difference in the paraelectric phase. Instead of decreasing, the relaxation rate here increases with increasing temperature and is much larger than in the bulk. The difference is due to self-diffusion in the “premelting state” induced by microconfinement. This also explains the previously observed giant growth of the dielectric permittivity of confined NaNO_2 more than 100 K below the melting temperature.

DOI: 10.1103/PhysRevB.70.132102

PACS number(s): 61.12.Ld, 61.46.+w, 77.84.Lf

I. INTRODUCTION

The experimental implementation of new effects in the physics of nanostructures relies upon our ability to create new types of structures and devices. Our understanding of material processing in the pursuit of ultrasmall structures is steadily advancing. Epitaxial growth and lateral microstructuring techniques have made it possible to create low-dimensional electronic systems with quantum-confined structures, i.e., quantum wells, quantum wires, and quantum dots. Nanostructures can also be obtained by confining a solid or a liquid within nanometer-sized pores of various porous materials. There are a lot of materials that incorporate in their structure systems of voids, i.e., nanometer pores. When we fill such a porous material with some substances, we may prepare certain types of nanostructures.

In particular, it is well known that the physical properties of ferroelectric materials in a restricted geometry strongly differ from those in the bulk.¹ A very remarkable result is the giant growth of the dielectric constant ϵ (up to 10^8 at 100 Hz) on approaching the bulk melting temperature ($T_M = 554$ K) of NaNO_2 embedded in an artificial matrix.² The giant growth of ϵ was tentatively attributed to the extremely broadened melting process, but no direct experimental evidence was given. A recent neutron-diffraction study³ of NaNO_2 embedded in a porous glass with a pore size of 7 nm showed that in the ferroelectric phase below $T_c = 437$ K the structure of the confined material is in good agreement with the one of bulk NaNO_2 ⁴ (space group Imm2). On heating through T_c to the paraelectric phase (Immm) a large growth of the amplitudes of thermal vibrations of all ions is observed leading to a “soft” premelting state³ with an increased unit-cell volume. In this case the growth of the dielectric permittivity of NaNO_2 above T_c could be tentatively explained by ionic currents due to jump diffusion of ions.

To check on this possibility and to throw some additional light on the differences between NaNO_2 in the bulk and in a confined geometry, we decided to perform a ^{23}Na spin-lattice relaxation study in the ferroelectric, as well as in the paraelectric, state.

II. RESULTS

Samples were prepared by the immersing the preliminary vacuum-annealed porous glass in the melted NaNO_2 for about 24 h in a sealed quartz container. The pore size distribution was checked by the mercury intrusion porosimetry and a peak at 7 nm with FWHM 2 nm has been found. The ^{23}Na ($I=3/2$) Larmor frequency was $\omega_L/2\pi = 100.523$ MHz and the Fourier transform spectra have been measured at 9 T. The solid echo pulse sequence has been used. The 90° pulse width was 3.6 μs . The central $\frac{1}{2} \rightarrow -\frac{1}{2}$ line has been irradiated. The magnetization decay could not be very well described by a single exponential decay, but a stretched-exponential form gave a satisfactory fit (Fig. 1).

The temperature dependence of the ^{23}Na spin-lattice relaxation rate (T_1)⁻¹ in bulk NaNO_2 obtained by Bonera *et al.*⁵

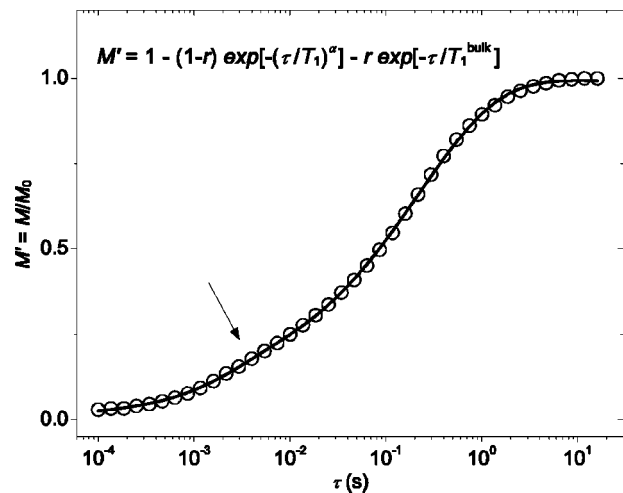


FIG. 1. Stretched-exponential fit of the ^{23}Na nuclear magnetization recovery plot in microconfined NaNO_2 at room temperature. The slight deviation (see arrow) from the stretched-exponential behavior is due to the bulk-like NaNO_2 component present in the cracks in the porous glass. It is accounted for by adding a second, exponential relaxation term to the magnetization recovery, with $r \sim 0.1$ – 0.15 denoting the volume fraction of the bulk component.

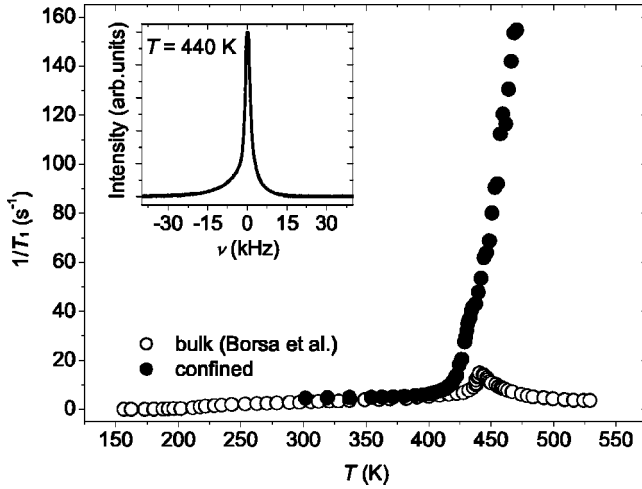


FIG. 2. Temperature dependence of the ^{23}Na spin-lattice relaxation rates of (a) bulk and (b) microconfined NaNO_2 . The observed shape of the $\frac{1}{2} \rightarrow -\frac{1}{2}$ ^{23}Na central transition is shown in the inset.

is compared in Fig. 2 with our data for microconfined NaNO_2 . The characteristic $(T_1)^{-1}$ anomaly at T_c in bulk NaNO_2 has disappeared in the confined system as the relaxation rate continues to increase on heating through T_c . In the microconfined NaNO_2 $(T_1)^{-1}$ is always larger than in the bulk. In the ferroelectric phase the relaxation rate $(T_1)^{-1}$ of the confined system increases with increasing T similarly as in the bulk. In the paraelectric phase, on the other hand, $(T_1)^{-1}$ in the confined system does not decrease with increasing T as in the bulk but continues to increase on heating. The inset to Fig. 2 shows the observed shape of the ^{23}Na central $\frac{1}{2} \rightarrow -\frac{1}{2}$ transition at $T = T_c^{\text{bulk}}$.

The basic result of this study is that microconfinement tremendously increases the sodium spin-lattice relaxation rate, i.e., the spectral density of the electric-field gradient (EFG) tensor \underline{V} fluctuations at the nuclear Larmor frequency ω_L ,

$$\left(\frac{1}{T_1}\right) \propto J(\omega_L) = K \int_{-\infty}^{+\infty} \langle \underline{V}(0)\underline{V}(t) \rangle e^{i\omega_L t} dt. \quad (1)$$

Assuming for the sake of simplicity that the correlation function of the EFG tensor decays exponentially, we find

$$\frac{1}{T_1} \propto \frac{\tau}{1 + \omega^2 \tau^2}. \quad (2)$$

Here, τ is the correlation time for EFG tensor fluctuations, which can be safely assumed to be Arrhenius-like,

$$\tau = \tau_0 e^{E/kT}. \quad (3)$$

At still higher temperatures between T_c and the melting temperature T_m , T_1 approaches T_2 as indeed expected for a melt. The T dependence of the stretched-exponential α and the spin-spin relaxation time T_2 is shown in Fig. 3.

III. DISCUSSION

Let us now try to determine the relaxation mechanism leading to the enhancement of the relaxation rate in the microconfined system.

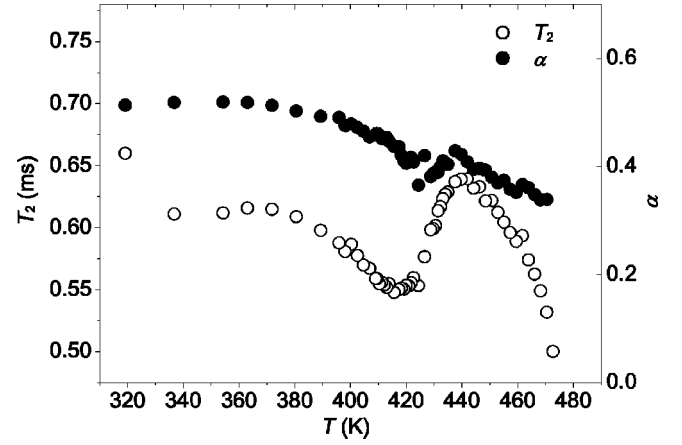


FIG. 3. Temperature dependence of the ^{23}Na spin-spin relaxation time T_2 and of the stretched exponent α of microconfined NaNO_2 .

In the bulk, the relaxation behavior is close to T_c determined by the ferroelectric soft mode⁵ and the corresponding fluctuations in the EFG tensor at the ^{23}Na site. This soft-mode contribution $(T_1^{-1})_{\text{sm}}$ is in confined NaNO_2 completely masked by another relaxation mechanism $(T_1^{-1})_{\text{mc}}$ characteristic of the microconfined “premelting state”³ and we can write

$$\frac{1}{T_1} = \left(\frac{1}{T_1}\right)_{\text{sm}} + \left(\frac{1}{T_1}\right)_{\text{mc}} \approx \left(\frac{1}{T_1}\right)_{\text{mc}}. \quad (4)$$

Let us now try to determine $(1/T_1)_{\text{mc}}$, i.e., the nature of the relaxation rate induced by the new mechanism characteristic for the microconfined system. It could reflect either the increase of the librations of the NO_2 groups detected by the neutron diffraction or sodium self-diffusion. A discrimination between these two mechanisms can be made on the basis of the temperature dependence of $(1/T_1)_{\text{mc}}$.

Since librations are certainly much faster than the nuclear Larmor frequency, we would be, in this case, in the fast motion limit and expression (4) would become

$$\frac{1}{T_1} \propto K\tau; \quad \omega_L \tau \ll 1. \quad (5)$$

This would mean that the relaxation rate decreases with increasing temperature instead of increasing as indeed observed. This rules out increased librations as the new rate-determining mechanism in the microconfined phase.

We thus have to find another mechanism with a characteristic inverse correlation time lower than the Larmor frequency, so that we are in the slow motion limit,

$$\frac{1}{T_1} \propto \frac{K}{\omega_L^2 \tau}; \quad \omega_L \tau \gg 1. \quad (6)$$

Such a mechanism could be EFG tensor fluctuations due to sodium self-diffusion. These are certainly slow and thermally activated, fulfilling the conditions of the validity of the above equation. Since the changes of the EFG produced by sodium jump diffusion among vacancy sites are large, as compared

to the changes produced by the atomic rearrangement at the ferroelectric transition, the self-diffusion mechanism can easily mask the mechanism valid in the bulk.

In this case we indeed have $\omega_1\tau \gg 1$, where τ is the characteristic time between ionic jumps. Thus, we obtain $(T_1)_{s.d.} \propto \tau$ and τ becomes shorter and shorter as temperature increases, leading to the observed increase of the relaxation rate.

The stretched exponent α defining the nuclear magnetization relaxation recovery shown in Fig. 3 continuously decreases with increasing temperature, reflecting a widening of the distribution of spin-lattice relaxation rates on going into the premelted state. The distribution in the relaxation rates is due to the distribution of sodium vacancy sites and pore sizes in the porous matrix, as well as to the random orientations of the EFG eigensystems at the sodium vacancy sites. The rather low values of α are due to the increased randomness of the system in the premelted state. The small dip in $\alpha(T)$ around $T=420$ K is connected with the smeared-out structural changes in the range of the ferroelectric phase transition.

The T dependence of T_2 can be understood by the same model as used for the interpretation of $T_1(T)$. This is so, as only the central ^{23}Na transition has been irradiated, for which T_1 and T_2 both measure only the spectral densities at the Larmor frequency and only differ in a numerical factor. The optical difference between Figs. 2 and 3 is due to the fact that in the former the relaxation rate $1/T_1$, and in the latter the relaxation time T_2 , has been plotted.

Let us now relate these results to the observed increase of the dielectric constant ϵ . The correlation time τ is related to the self-diffusion constant D via

$$D = \frac{\lambda^2}{\tau}, \quad (7)$$

where λ is the mean jump distance. The conductivity σ of the system is, on the other hand, related to the diffusion constant D by

$$\sigma = \frac{nq^2D}{kT}, \quad (8)$$

where n is the density of the charge carriers (i.e., sodium vacancy density), q is the effective charge, k is the Boltzmann constant, and T is the temperature.

The increase of the conductivity results in the strong increase of the imaginary part of the dielectric permittivity and consequently, via the Kramers-Kronig relations, also of the real part. The frequency dependence of the dielectric constant is characteristic for the Maxwell-Wagner effect (see, e.g., Ref. 6). A more elaborate treatment performed for the case of the so-called "dielectric anomaly of rocks"⁷⁻¹⁰ demonstrated that in the case of the porous dielectric material filled with the conducting one, the real part of the dielectric constant can grow to very large values (of about 10^6).

We can thus conclude that the increase of the sodium spin-lattice relaxation rate in the confined system reflecting the shortening of τ is due to increase of the sodium self-diffusion constant.

ACKNOWLEDGMENTS

This work was supported by the Slovenia-Russia Bilateral Program, RFBR (Grant Nos. 04-02-16550 and 01-02-17739) and INTAS-2001-0826.

*Electronic address: s.vakhrushev@mail.ioffe.ru

¹W. L. Zhong, Y. G. Wang, and P. L. Zhang, *Ferroelectr. Rev.* **1**, 131 (1998).

²S. V. Pan'kova, V. V. Poborchii, and V. G. Solov'ev, *J. Phys.: Condens. Matter* **8**, L203 (1996).

³A. V. Fokin, Y. A. Kumzerov, N. M. Okuneva, A. A. Naberezhnov, S. B. Vakhrushev, I. V. Golosovsky, and A. I. Kurbakov, *Phys. Rev. Lett.* **89**, 175503 (2002).

⁴M. I. Kay, *Ferroelectrics* **4**, 235 (1972).

⁵G. Bonera, F. Borsa, and A. Rigamonti, *Phys. Rev. B* **2**, 2784 (1970).

⁶C. Kittel, *Introduction to Solid State Physics*, 5th ed. (Wiley, New York, 1976), p. 430.

⁷P. N. Sen, *Appl. Phys. Lett.* **39**, 667 (1981).

⁸P. Z. Wong, J. Koplik, and J. P. Tomanic, *Phys. Rev. B* **30**, 6606 (1984).

⁹F. Brouers and A. Ramsamugh, *J. Phys. C* **21**, 1839 (1988).

¹⁰F. Claro and F. Brouers, *Phys. Rev. B* **40**, 3261 (1989).